E. Fixed Bed Studies with Developmental Catalyst SG-B-2

1. Task 1 - Exploratory Process Research

Three feed compositions were used in these studies. They were 1/1 H_2/CO, 2/1 H_2/CO, and another, essentially 1/1 H_2/CO diluted with carbon dioxide and methane. The composition of the third feed, 0.9 $H_2/CO/0.3\ CO_2/3.4\ CH_4$, approximated a practical feed, with recycle, for a fixed fluidized-bed operation with SG-B-2. Problems related to temperature control were encountered with this catalyst in the bench-scale fixed-bed unit, and it was removed from the program before micro reactor studies were completed. Results obtained prior to this are discussed below.

a. Activation of Catalyst SG-B-2

Activation of catalyst SG-A-1 was done in flowing hydrogen at 950°F, and always gave a high activity catalyst. However, SG-B-2 was not as active as SG-A-1, and a series of experiments were made using flowing hydrogen at temperatures between 500 and 950°F to determine the optimum activation temperature for catalyst SG-B-2. The data are given in Table C1 of Appendix C using the methane diluted charge stock (0.9 $H_2/1.0\ CO/0.3\ CO_2/3.2\ CH_4$). Scatter occurred in the selectivity data due to the high methane content of the feed. However, based on activity for carbon monoxide conversion, nothing was gained by hydrogen pretreatment at temperatures above 600°F. Product quality was the same for all runs.

b. Effect of Charge Stock on SG-B-2 Performance

The data obtained while processing H_2/CO, $2H_2/CO$ and 0.9 $H_2/CO/0.3\ CO_2/3.4\ CH_4$ are presented in Tables C2-C5 of Appendix C, and discussed below.

H_2/CO

Preliminary experiments (Table C1) indicated that 66 to 68% of the stoichiometric amount of carbon monoxide could be converted at 507°F, 200 psig, and a contact time of 20 seconds. The C_5+ liquid hydrocarbon product obtained is highly branched and has an 87 R+0 octane number.

Temperature effects at 200 psig and 20 seconds contact time were studied between 485°F and 600°F (Table C3). An upper process temperature limit of approximately 525°F must be maintained, as C_5+ gasoline selectivity drops dramatically at higher temperatures. At 525°F, the CO conversion is also satisfactory (38% or 76% of theory). Below 500°F, the conversion falls to <30%, thus, resulting in a narrow window for operating this catalyst with H_2/CO. These points are illustrated in Figures 23 and 24.

Figure 23

EFFECT OF TEMPERATURE ON ACTIVITY OF SG-B-2

(200 psig, $H_2/CO = 1$ and $\tau = 19.8$ sec)

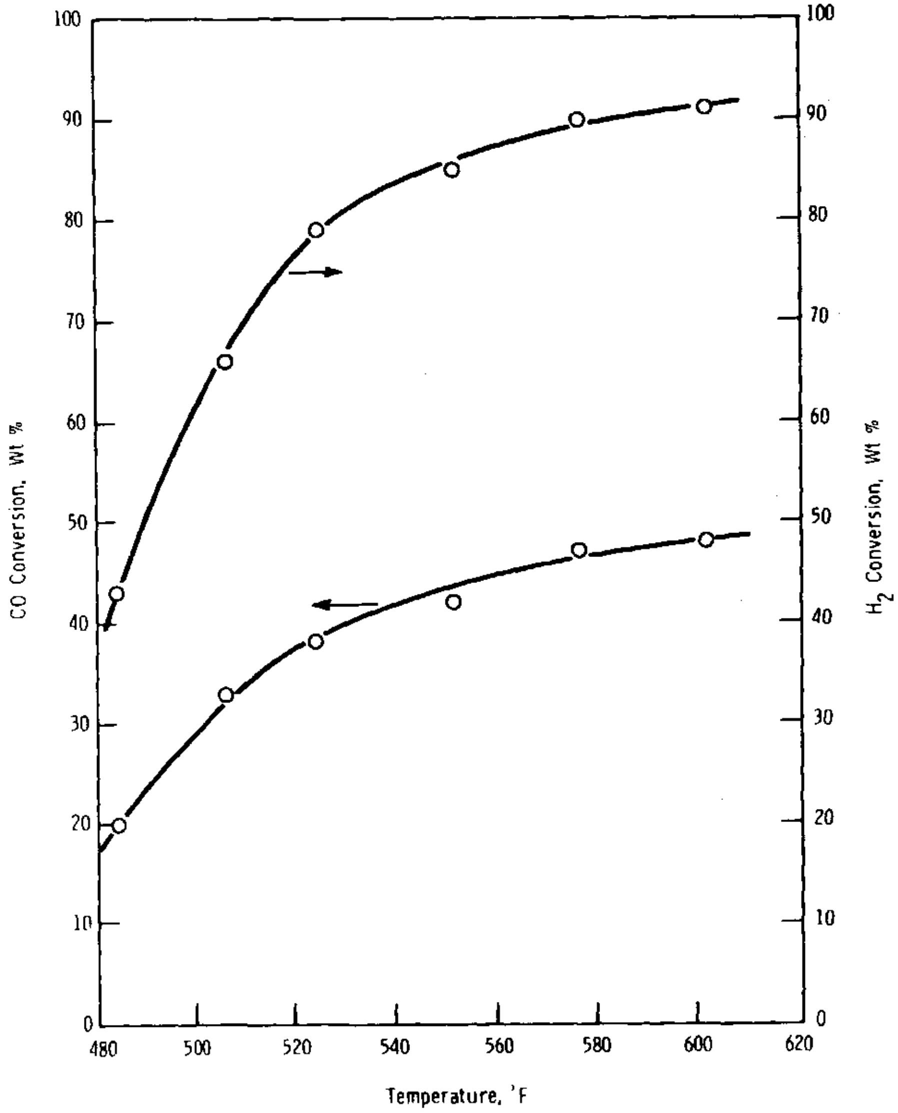

Figure 24

EFFECT OF TEMPERATURE ON HYDROCARBON SELECTIVITY WITH SG-B-2

(200 psig, $H_2/CO = 1$ and $\tau = 19.8$ Sec.)

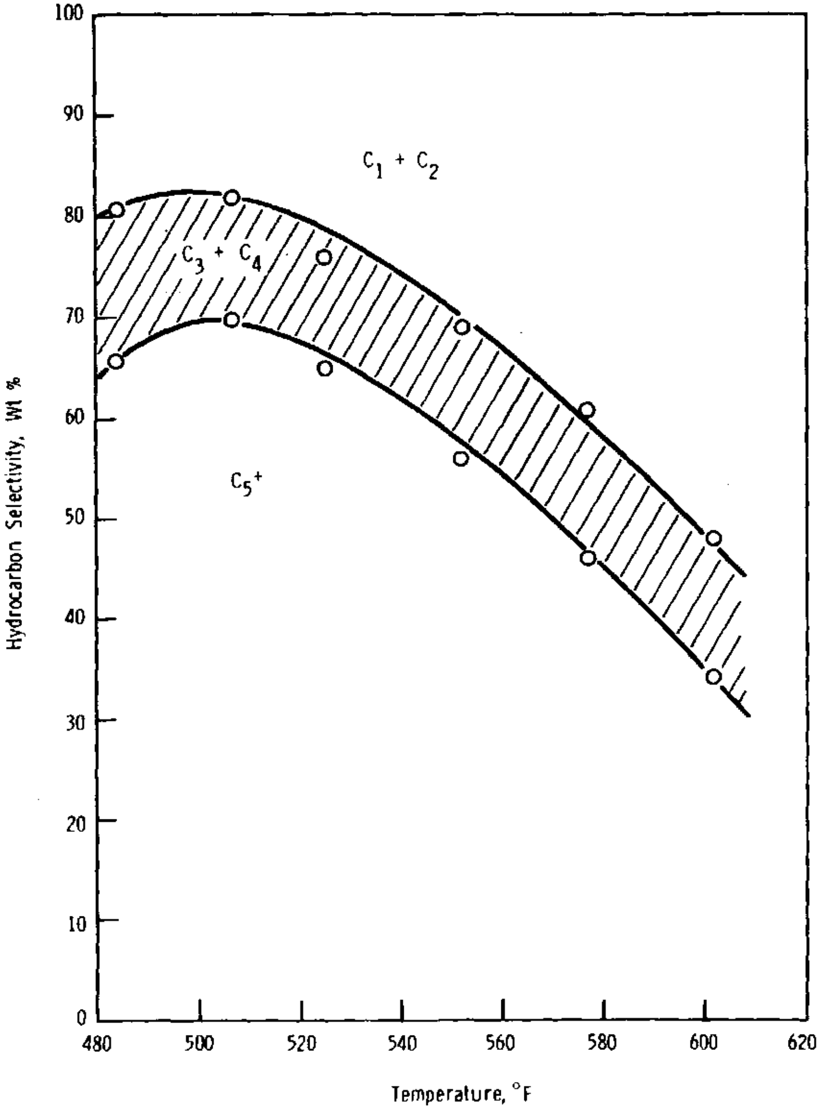

$2H_2/CO$

A comparison of SG-B-2 performance between charges H_2/CO and $2H_2/CO$ (Table 21) showed the expected increase in CO conversion with the hydrogen rich charge. Note, however, the CO conversion is about the same percent of theory in either case. The selectivity to C_1+C_2 is smaller and the C_5^+ selectivity is greater for the H_2/CO charge compared with the $2H_2/CO$. Both charges yield a C_5^+ product with a 90% overhead boiling point of <400°F.

$0.9\ H_2/CO/0.3\ CO_2/3.4\ CH_4$

Data obtained with this charge at 525°F and 100 and 200 psig and varying contact times are shown in Table C5. The low, <1%, selectivity to methane is not real and was attributed to problems in analyzing for small, additional amounts of methane over that in the charge. Note the 40 to 65% selectivity to C_6^+ aromatics compared with about 15% obtained at comparable conditions with a H_2/CO charge. These data may be misleading, as the aromatic selectivity in the total hydrocarbon produced with $0.9/CO/0.3\ CO_2/3.4\ CH_4$ is only 1.5 times that obtained with H_2/CO (c.f. run 58-7, Table C3 with 59-1, Table C5). Nevertheless, the higher aromatic selectivity can be expected to age the catalyst more rapidly.

Figure 25 shows plots of activity data selected to minimize aging effects of the catalyst. The conclusion drawn is that at the same contact time, there is no effect upon catalyst activity despite differences in operating pressure between 100 and 200 psig.

c. Effect of Carbon Monoxide Partial Pressure

Process studies have revealed significant effects by diluting a 1/1 H_2/CO charge with CO_2 and CH_4. This diluted charge ($0.9\ H_2/CO/0.3\ CO_2/3.4\ CH_4$), approximates the combined feed for a fixed fluidized bed operation, and gives a hydrocarbon product containing significantly less methane and less C_5^+ gasoline, as well as enhanced aromatics formation, when compared with H_2/CO as charge (Table C6). The data are summarized in Table 22. The diluted charge apparently favors C_2-C_4 formation at the expense of C_1 and C_5^+. It is recognized that analytical problems can greatly affect apparent selectivities, due to the large amount of methane in the charge. Nevertheless, the enhanced aromatic and C_2-C_4 contents were significant enough to warrant several runs to resolve the differences. These runs were made at conditions such that the carbon monoxide partial pressures and space velocities would be equal for the two charge stocks. This necessitated running the 1/1 H_2/CO at a CO partial pressure of 28 psia and 270 GHSV and the diluted charge at 107 psia and 728 GHSV on CO.

TABLE 21

COMPARISON OF CATALYST SG-B-2 PERFORMANCE WITH H_2/CO AND $2H_2/CO$

Run 158-99-	2	3	5	6
Charge, H_2/CO	1/1	1/1	2/1	2/1
Temperature, °F	500	518	498	515
Contact Time, sec.	20	20	20	20
Conversion				
CO	35	39	63	71
H_2	64	75	66	78
Selectivity				
C_1+C_2	15	21	24	28
C_3+C_4	12	14	13	13
C_5+	73	65	63	49
90% OH, °F	393	380	393	362

TABLE 22

EFFECT OF CHARGE STOCK ON HYDROCARBON SELECTIVITY$^{(a)}$

Charge, $H_2/CO/CO_2/CH_4$	1/1/0/0	0.9/1/0/0.3/3.4
Conversion, wt %		
CO	38	32
H_2	79	85
Selectivity, wt %		
C_1	21	6
C_2	2	16
C_3+C_4	11	36
C_5+	65	42
Olefins in C_5, wt %	64	7
Aromatics in C_6^+, wt %	17	45

(a) 525°F, 200 psig and 1500 GHSV.

Figure 25

EFFECT OF CONTACT TIME ON ACTIVITY
OF SG-B-2 AT 525° F

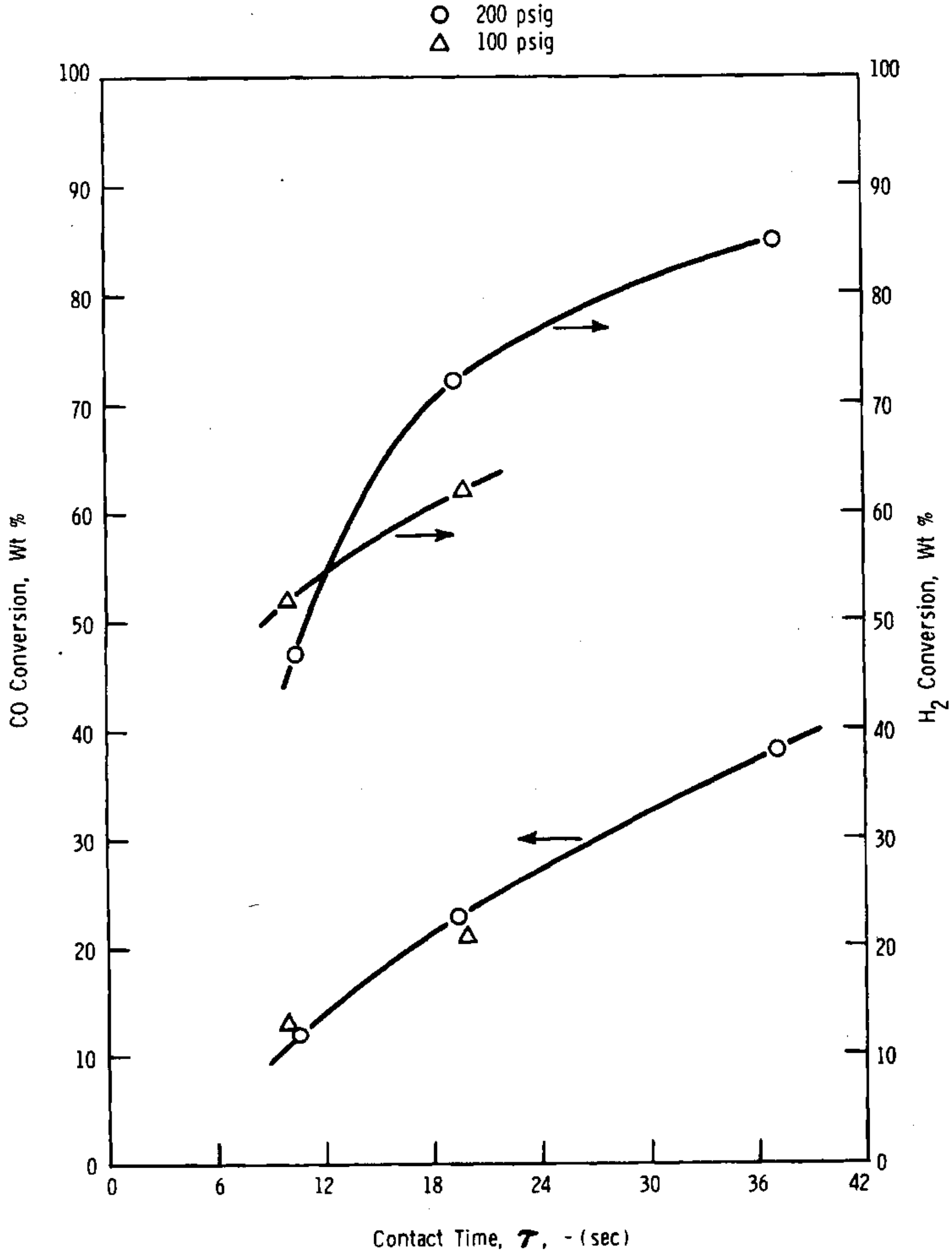

The low pressure runs (Table C6) with the 1/1 H_2/CO charge simulated the carbon monoxide space velocity and partial pressures used earlier with the dilute charge (Table 23). The results become more consistent at equal CO partial pressures. The H_2/CO charge made considerably more aromatics, 55% versus 17%, at 200 psig (107 psia $\overline{pp}$ CO), and fewer olefins. However, the hydrocarbon selectivities indicate that other factors may be important. Despite the equivalence of the C_5^+ gasoline selectivities, the dilute charge yielded less light gas and more C_3-C_4. This could just be a total pressure effect, as some earlier work with catalyst SG-A-1 showed quite poor C_5^+ selectivities at 50 and 100 psig pressures.

Likewise, increasing the pressure of the dilute charge made the results for the two charge stocks more consistent (Table 23). The diluted charge made less aromatics and more olefins at 540 psig than at 200 psig, but they still differ from the 1/1 H_2/CO charge. More C_5^+ gasoline is made at the higher pressure (for the dilute charge), but the dilution still gives a vastly different C_1-C_4 distribution. The lowered methane and increased C_4 selectivities appear inherent with the diluted charge for this catalyst.

With both charge stocks, halving the space velocity and decreasing temperature to 485°F gave enhanced C_5^+ gasoline production, more olefin, less aromatics, and a somewhat higher boiling product (Table 24). It also made the C_4^- product slates for the charge stocks more equivalent. The enhanced C_2-C_4 yield for the dilute charge, however, is still quite apparent.

To further investigate effects of dilution, runs were made with nitrogen replacing methane, and with carbon dioxide eliminated from the charge. Selected data from Tables C7, C8 and C9 are given in Table 25 to summarize the dilution effects at 200 psig total pressure, 485°F and about 700 GHSV. Within analytical accuracies, substituting nitrogen for methane, or eliminating CO_2, had no effect on the catalyst performance. Dilution favors C_2-C_4 hydrocarbons at the expense of gasoline and yields more aromatics. As discussed in the early part of this section, partial pressure and space velocity of CO partially explain the difference.

d. Aging and Regeneration of SG-B-2

Initial aging studies with catalyst SG-B-2 utilized the dilute charge (0.9 $H_2/CO/0.3\ CO_2/3.4\ CH_4$). Charge rate at 485°F was 770 GHSV, while at 525°F, the rate was increased to 1500 GHSV to give approximately the same initial catalyst activity for both runs (see Tables C10 and C1, respectively). The milder conditions showed slower aging (Figure 26), while converting more CO after 9 days than did the higher rate during 4.5 days (4.5 days at 1500 GHSV, is equivalent to 9 days and 770 GHSV, with respect to the total carbon monoxide passing over the catalyst).

TABLE 23

COMPARISON OF H_2/CO AND DILUTED H_2/CO AT THE SAME CO PARTIAL PRESSURE AND GHSV

Run No.	159-136	143-59-1	143-58-7	158-101
Charge, $H_2/CO/CO_2/CH_4$	1/1/0/0	0.9/1.0/0.3/3.4	1/1/0/0	0.8/1.0/0.2/3.1
Pressure, psig	60	200	200	540
pp CO, psia	37	38	107	109
GHSV on Total Charge	557	1511	1457	4572
GHSV on CO	274	270	728	896
Conversion, wt %				
CO	39	32	38	30
H_2	77	85	79	69
HC Selectivity, %				
C_1	38	6	21	9
C_2	3	16	2	13
C_3+C_4	20	36	11	26
C_5^+	39	42	65	52
Olefin in C_5, wt %	8	7	64	37
Aromatics in C_6^+, wt %	55	45	17	30

TABLE 24

EFFECT OF DILUTION AT LOWER TEMPERATURE AND LOWER GHSV

Run No.	143-58-7	158-102-3	143-59-1	143-60-2
Charge, $H_2/CO/CO_2/CH_4$	1/1/0/0	1/1/0/0	0.9/1.0/0.3/3.4	0.9/1.0/0.3/3.2
Temperature, °F	525	485	528	485
Pressure, psig	200	200	200	200
$\overline{pp}$ CO, psia	107	107	38	40
GHSV Total	1457	720	1511	772
GHSV on CO	728	360	270	143
Conversion, wt %				
CO	38	35	32	30
H_2	79	68	85	76
Selectivity, wt %				
C_1	21	15	6	15
C_2	2	2	16	11
C_3+C_4	11	11	36	25
C_5+	65	72	42	49
Olefins in C_5, wt %	64	76	7	21
Aromatics in C_6^+, wt %	17	8	45	39
90% OH, °F	367	396	356	372

TABLE 25

COMPARISON OF METHANE AND NITROGEN DILUTION ON CATALYST SG-B-2 PERFORMANCE

Run No.	158-102-3	143-60-2	143-63-1	159-137-2
Charge, $H_2/CO/CO_2/CH_4$	1/1/0/0	0.9/1.0/0.3/3.2	-	0.9/1/0/3.1
$H_2/CO/CO_2/N_2$	-	-	0.9/1.0/0.3/3.5	-
$\overline{pp}$ CO, psia	107	40	35	40
GHSV on CO	360	143	116	156
Conversion, wt %				
CO	35	30	36	35
H_2	68	76	86	81
Selectivity, wt %				
C_1	15	15	16	22
C_2	2	11	3	8
C_3+C_4	11	25	25	15
C_5+	72	49	56	55
Olefins in C_5, wt %	76	21	14	24
Aromatics in C_6+, wt %	8	39	35	28

Figure 26

AGING STUDIES WITH CATALYST SG-B-2

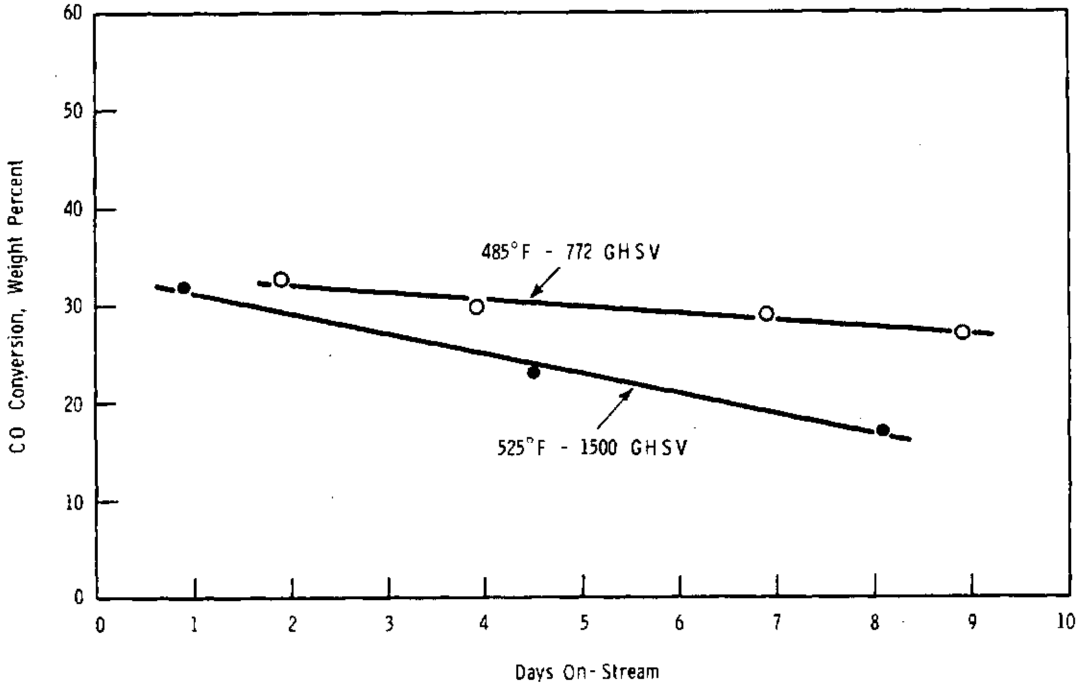

Figure 27

AGING RATE OF CATALYST SG-B-2 BEFORE AND AFTER OXIDATIVE REGENERATION

(525°F, 200 psig and 1500 GHSV)

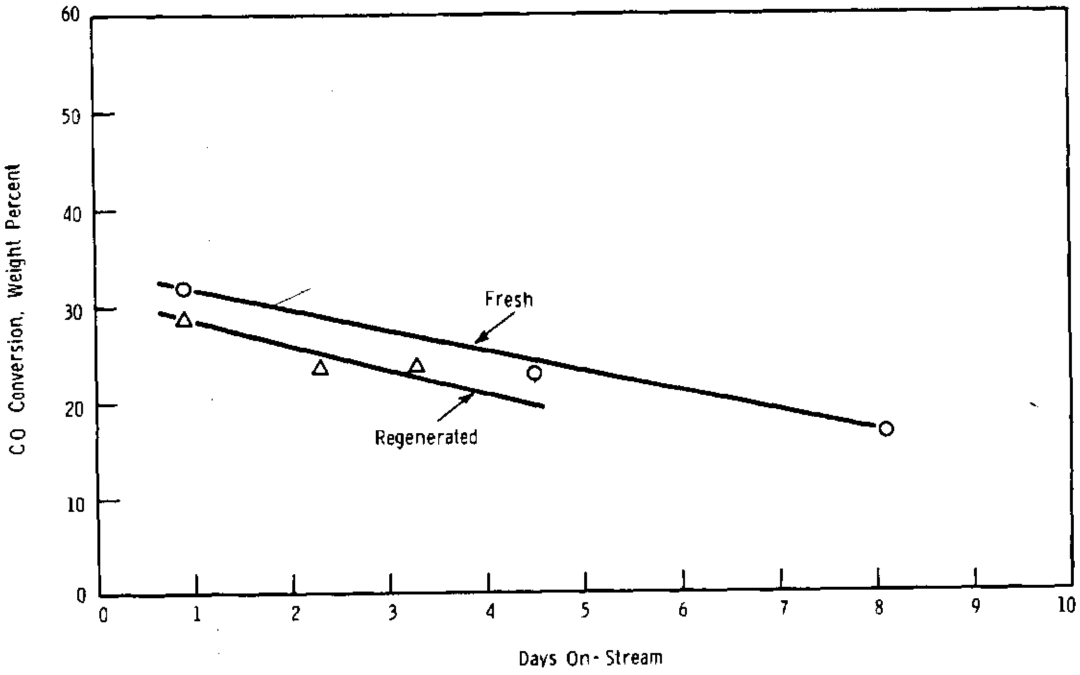

After processing nine days at 485°F, the catalyst was oxidatively regenerated with an initial burn at 750°F, using 3.5% oxygen in nitrogen, and a final burn at 950°F with 8.5% oxygen in nitrogen for 19 hours. The results (Figure 27) show identical aging rates, with a loss of initial activity from 33 to 29% (Table C11).

A hydrogen regeneration of aged SG-B-2 also showed this same activity loss in second cycle operation, with CO conversion decreasing from 35 to 29% (Tables C11 and C1).

Aging runs were also made with H_2/CO. Following activation in flowing hydrogen at 600°F and 200 psig for 16 hours, experiments were carried out at 485°F, 200 psig, and 700 GHSV. Both hydrogen and air regenerations of the catalyst were attempted.

The air regeneration procedure consisted of an initial burn for one hour at 750°F with 1% oxygen in nitrogen at 100 psig. The temperature was then raised to 850°F and held for one hour. The catalyst was next contacted with 100% air and when no further indications of burning were observed, the temperature was raised to 900°F. Two hours at 900°F with 100% air was the final condition of the regeneration procedure. After each air regeneration and before contacting with synthesis gas, the catalyst was given a hydrogen pretreatment for 16 hours at 600°F and 200 psig.

The activity and hydrocarbon selectivity as a function of time on stream are shown in Figures 28 and 29, respectively (Table C12).

Catalyst activity for carbon monoxide conversion (Figure 28 ①) fell from 36% at six days to 30% after 18 days of processing. Thus, after 18 days on stream, 60% of the stoichiometric quantity of carbon monoxide was being converted. The C_5^+ hydrocarbon selectivity remained high throughout the run, and the liquid product had a constant research octane number of 89.

	Days On Stream	
Hydrocarbon, wt %	6	18
$C_1 + C_2$	15	20
$C_3 + C_4$	9	14
C_5^+	76	66
C_6^+, Aromatics	8	6
Liquid O.N. (R+0)	89	89

Further, the C_6^+ aromatic make was 10% and C_5 olefin selectivity >70%, with equilibrium amounts of branched C_5 olefins being formed.

After the initial aging curve, the temperature was raised from 485 to 505°F. The effect was to increase carbon monoxide conversion from 30 to 36%.

Figure 28

AGING AND REGENERATION STUDY ON CATALYST SG-B-2

GHSV = 775
H_2/CO = 1
Press = 200 psig
Temp = 485°F

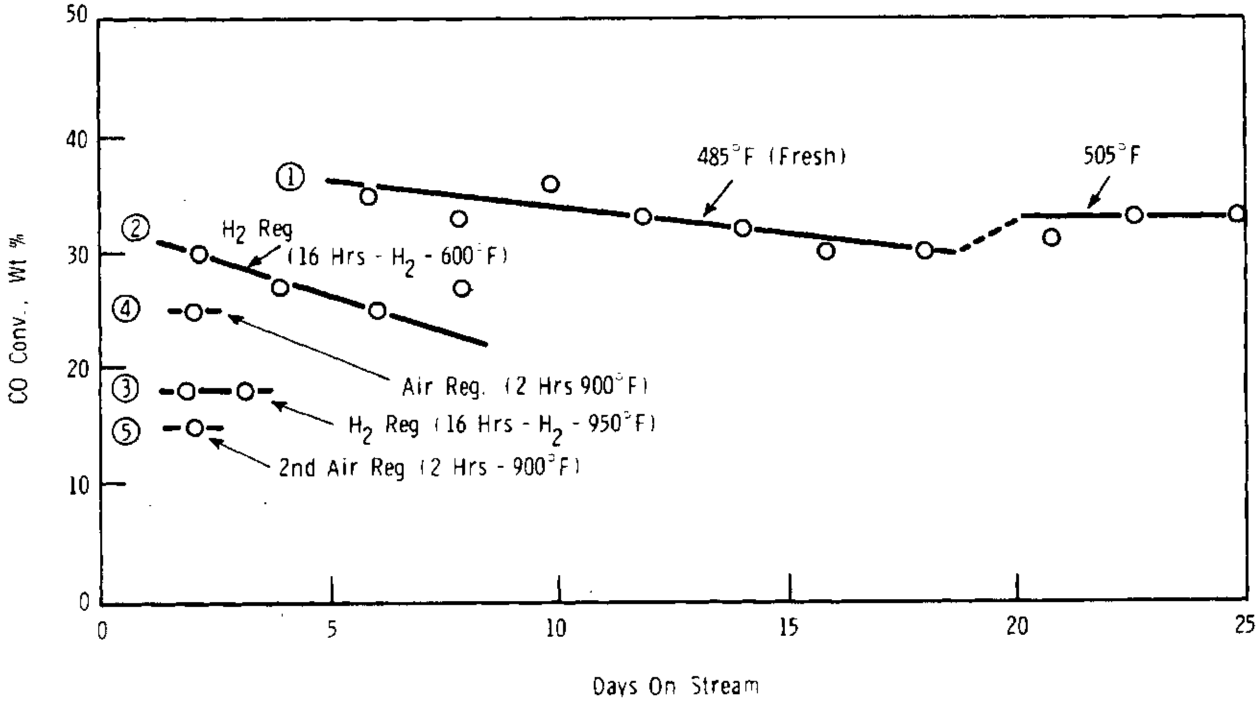

Figure 29

HYDROCARBON SELECTIVITY WHILE AGING CATALYST SG-B-2
(H_2/CO; 485 F; 200 psig; GHSV 700)

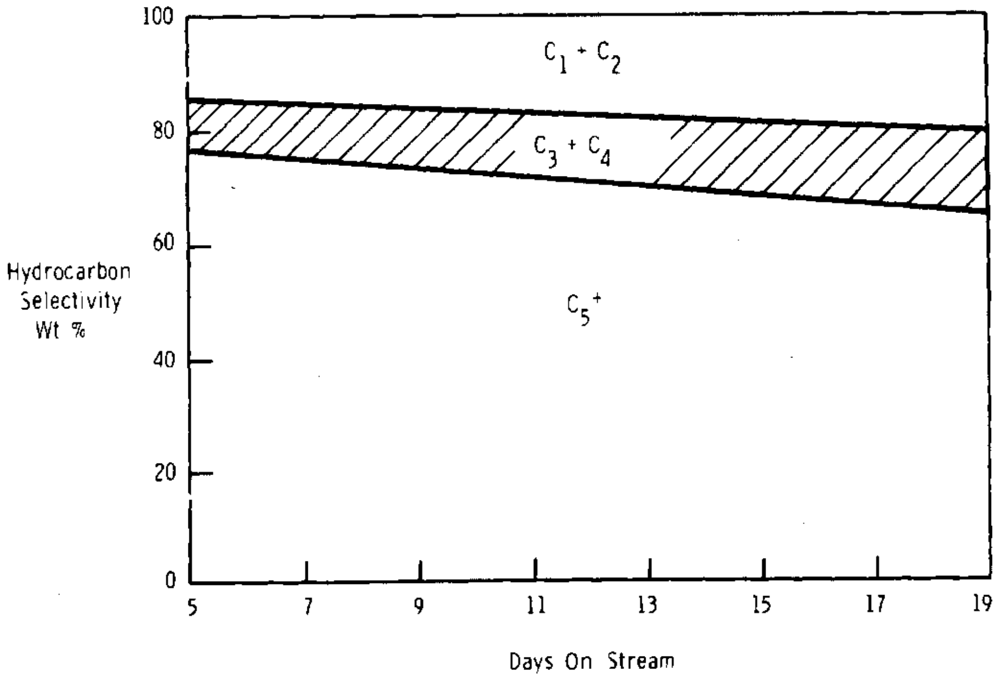

Hydrogen regeneration (Figure 28 - ②) of the catalyst for 16 hours at 600°F, was not successful. Six days of conversion data, before and after H_2 regeneration, showed a drop from 35 to 25% carbon monoxide converted. Increasing the severity of H_2 regeneration to 16 hours at 950°F (Figure 28 - ③) resulted in a further loss in activity to only 18% CO converted. An air regeneration (Figure 28-④) increased activity for CO conversion from 18 to 25%. A second air regeneration at the same conditions (2 hr-air-900°F) resulted in a catalyst of much lower activity (15% CO conversion).

The data indicate that, although SG-B-2 initially has good aging characteristics, it did not regenerate under the conditions employed.

2. Task 2 - Process Development

Based on preliminary results with developmental catalyst SG-B-2 in the micro reactor units, a bench-scale unit experiment was started at the following conditions:

Fresh Feed	2.2 H_2/CO/0.5 CH_4
GHSV, Fresh Feed	325
Pressure, psig	300
Inlet Temperature, °F	400
Maximum Temperature, °F	500
Recycle Ratio	14/1

After a short time on stream, it became necessary to increase the inlet and maximum temperatures to 425° and 525°F, respectively, in an attempt to obtain steady conditions. Some problems were also encountered in obtaining the desired H_2/CO ratio in the fresh feed. Material balances for this run, 225-15, are shown in Table C13.

After about 97 hours on stream, the total conversion (H_2+CO) was 88% at a H_2/CO ratio of 2.6/1. However, the selectivity to C_5^+ gasoline was only 36% and the C_5^- fraction was almost exclusively paraffinic. As the fresh feed H_2/CO ratio was brought closer to 2.2, the H_2+CO conversion dropped to about 75% and the C_5^+ gasoline selectivity increased to 47-50%. Methane was the predominant light hydrocarbon, and olefin production remained low.

After two weeks of operation, the GHSV on fresh feed was doubled in an attempt to improve the selectivity to gasoline and olefins. The H_2+CO conversion fell to about 40-45% with no improvement in the production of olefins. Actually, the selectivity to gasoline decreased to about 40% while that to methane increased slightly. The lower conversion at the higher space rate permitted a reduction in the recycle ratio to 9.5/1.

The space velocity was reduced to the original condition (i.e., 330 GHSV on fresh feed) at about the 19th day, to determine any significant effects of catalyst aging. The H_2+CO conversion was not significantly different. However, differences in the hydrocarbon selectivities were apparent. More methane, >40%, and less gasoline, <40%, were made.

After about 28 days, run 225-15 was interrupted by a power failure. Subsequent operation of the bench-scale unit was erratic and the run was, therefore, terminated. The space velocity history of run 225-15 was:

GHSV on Fresh Feed	Days On Stream
325	12
650	5
325	14

Run 225-16 was started with a fresh charge of catalyst SG-B-2 at the following conditions:

Fresh Feed	2.1 H_2/CO/0.5 CH_4
GHSV, Fresh Feed	325
Inlet Temperature, °F	425
Maximum Temperature, °F	525
Pressure, psig	300
Recycle Ratio	13/1

The results of two material balances (225-16-1 and -2) at these conditions are given in Table 26. The H_2+CO conversions are both approximately 88-90 mole %. The C_5^+ yields are 54-61 wt % of total hydrocarbons. The C_4^- fractions consist of about 50% methane (wt % basis), and the remainder primarily C_2-C_4 paraffins. The C_5 fractions are essentially paraffinic (iso to normal ratio about 1.6/1). The C_6^+ fractions contain about 50 wt % paraffins and about 30 wt % aromatics.

The recycle ratio during material balances 225-16-1 and -2 was 12.5/1. The H_2/CO ratios in the recycle gases were 1.6/1 and 1.8/1, respectively.

The composition of the fresh feed was then changed to 1.5 H_2/CO/0.5 CH_4 in an attempt to improve olefin and perhaps gasoline selectivity. Material balance 225-16-3 was obtained after the unit had appeared to stabilize at this new feed composition (with a recycle ratio of 9/1). However, during the next material balance (225-16-4), severe temperature fluctuations in the reactor were observed. Attempts to reduce or eliminate these temperature oscillations by altering the recycle ratio were unsuccessful. Therefore, both the reactor inlet temperature and maximum temperature were increased by about 10°F. By careful adjustment of the recycle ratio (about 18/1) and close observation of other operating variables, the unit became reasonably stable.

TABLE 26

MATERIAL BALANCES FROM FIXED BED BENCH-SCALE UNIT WITH CATALYST SG-B-2

RUN NUMBER 225-	16- 1	16- 2	16- 3	16- 4	16- 5	16- 6	16- 7	16- 9
RUN DAYS-ON-STREAM	1.9	2.9	5.7	6.8	9.7	10.7	11.8	13.7
CUM. DAYS-ON-STREAM	1.9	2.9	5.7	6.8	9.7	10.7	11.8	13.7
FRESH FEED H2/CO RATIO	2.3	2.4	1.5	1.5	1.4	1.4	1.4	1.4
GHSV, HR^{-1}	327	332	298	298	293	298	298	300
RECYCLE RATIO	12.46	12.63	9.29	9.10	17.91	18.57	18.14	18.25
REACT. PRESS., PSIG	300	300	300	301	304	300	300	300
REACT. INLET TEMP., °F	423	424	423	424	436	438	435	437
NOM. REACT. TEMP., °F	488	487	498	506	500	499	467	493
CONVERSIONS, MOL °/°								
H2	90.4	88.8	79.3	76.0	75.7	72.5	66.8	62.6
CO	88.2	84.9	55.6	49.6	48.9	47.2	41.6	39.3
H2+CO	89.7	87.6	69.7	65.5	64.6	61.9	56.3	52.9
YIELDS, WT °/°								
HYDROGEN	1.4	1.7	2.0	2.4	2.3	2.5	3.1	3.5
WATER	48.8	49.8	29.9	28.9	26.8	25.0	23.0	22.3
CO	10.2	12.9	40.5	45.8	46.7	48.4	53.5	55.5
CO2	1.2	0.9	1.0	0.8	2.2	1.9	1.6	1.4
TOTAL HYDROCARBON	38.4	34.6	26.7	22.1	22.0	22.2	18.8	17.3
HC SELECTIVITY, WT °/°								
METHANE	24.1	17.0	22.8	18.7	30.1	31.3	30.1	33.9
ETHENE	0.0	0.1	0.1	0.1	0.1	0.1	0.1	0.1
ETHANE	3.6	3.3	2.3	2.2	2.4	2.6	2.9	3.2
PROPENE	0.2	0.1	0.2	0.2	0.2	0.2	0.3	0.3
PROPANE	6.3	6.2	4.9	4.1	5.9	5.4	5.2	5.0
BUTENES	0.1	0.2	0.7	1.1	1.0	0.4	0.5	0.4
I-BUTANE	6.2	5.9	5.2	4.5	7.0	6.0	5.7	5.3
N-BUTANE	5.5	5.9	4.7	4.0	5.2	4.8	5.0	4.7
TOTAL C4-	45.9	38.6	40.8	35.1	51.9	50.8	49.7	52.9
C5+ PARAFFINS	24.0	29.5	21.6	25.3	19.8	20.4	21.1	19.4
OLEFINS	5.3	7.6	11.6	14.2	6.4	5.2	5.3	5.7
NAPHTHENES	3.6	4.0	2.3	2.9	3.0	2.8	2.5	2.2
AROMATICS	12.2	9.4	7.9	2.4	13.2	7.2	11.3	10.4
OTHERS	9.1	10.9	15.7	20.2	5.7	13.5	10.1	9.3
TOTAL C5+	54.1	61.4	59.2	64.9	48.1	49.2	50.3	47.1
YIELDS, G/SCM CONV CO+H2								
TOTAL HC	188	168	212	184	193	204	190	185
C5+	101	103	125	120	93	100	95	87
OLEFINS, WT °/° BY C NO.								
C2	1.3	1.6	3.9	5.9	4.4	4.3	4.3	4.3
C3	2.4	2.1	3.1	5.1	3.2	3.7	4.7	5.6
C4	0.9	2.0	6.7	11.7	7.3	3.9	4.4	3.8
C5	2.6	5.4	13.9	22.6	3.3	7.6	7.9	8.6
90 PCT OH, RAW PROD., °F	376	383	395	409	382	383	388	400
OCTANE NO. ON RAW PROD.								
R+O	84.5	83.4	84.9	85.6	89.0	89.5	88.2	87.5
R+3	-	-	-	-	-	-	-	-
OXYGENATES, WT °/°	0.1	0.1	-	-	-	-	-	-

Comparison of the third material balance with the first two balances illustrates the effects of the lower H_2/CO ratio in the fresh feed on conversion and product selectivities. As expected, carbon monoxide conversion decreased sharply and hydrogen conversion was about 10 wt % lower. Of course, the yields of hydrocarbons and water were correspondingly lower while more olefins were formed in the third balance.

The composition of the recycle gas was strongly influenced by the H_2/CO ratio of the fresh feed. The H_2/CO ratio in the recycle gas of balance 3 was 0.6/1 in contrast to about 1.7/1 in the first two balances.

The results of material balances 225-16-5, -6, -7, and -9 are also included in Table 26. They were obtained at slightly higher reactor temperatures than the third material balance. Also, the recycle ratio was approximately 18/1 (compared to 12/1 in balance 3). In these four balances, the yield of methane was higher, and less C_5^+ was obtained. Also, less olefins were formed. The isoparaffins (about 70 wt %) in the C_5 fraction of balance 5 appear to be unusually high.

After the ninth material balance, the pressure was raised to approximately 580 psig. However, large temperature fluctuations occurred in the reactor at this higher pressure. All attempts to eliminate these fluctuations by adjusting the recycle ratio and reactor temperatures were futile. In addition, a pressure drop of 40 psig developed across the reactor (probably related to the high catalyst temperatures). Run 225-16 was, therefore, terminated.

The research octane numbers (RON) of the hydrocarbon condensates from material balances 225-16-1, -2, and -3 are about 83-85, and those from 225-16-5, -6, -7 and -9 are higher (i.e., 87.5 to 89.5).

Simulated (gas chromatographic) distillations of the raw product show 90% overhead cut points of about 380°F for the first two runs, which had relatively high H_2/CO ratios. When the space velocity was lowered for balance 3, the 90% point rose to 395°F. It dropped again to 382°F when the maximum reactor temperature was raised about 20°F, and finally rose slowly to 400°F as the catalyst aged.

A sample of the aqueous phase from material balance 225-16-9 was analyzed for oxygenates. It contained about 0.2 wt % non-acidic organic compounds, which are listed below:

Compound	Relative Concentration[a] wt %
C_1-C_4 Aldehyde	2.5
Acetone	25.3
Methylethyl Ketone	8.3
Methylpropyl Ketone	1.1
Methanol	53.7
Ethanol	0.7
Propanol	1.3
Butanol	7.1

(a) Water-free basis

Two different types of fixed bed catalyst (SG-A and SG-B) were studied in the fixed bed, adiabatic bench-scale unit. As expected, high recycle ratios, which are an economic disadvantage in commercial operation, were required to control reactor temperatures for the exothermic syngas conversion process. Wide-temperature fluctuations and unsteady operation were observed. In addition, reactor plugging problems were encountered. Because of these and other considerations, operation under the fixed-bed mode was terminated.

F. Task 4 - Theoretical Studies in Support of Process Research with Fixed Bed Catalysts

1. Heat and Mass Transfer between Catalyst and Gas Stream

During synthesis gas conversion, about 5000 BTU's are released per pound of hydrocarbon formed. All this heat is generated within the catalyst and transferred to the bulk gas stream. The heat transfer is driven by the temperature difference between the catalyst surface and the bulk gas stream. The magnitude of the temperature difference depends on the reaction rate (which is a function of catalyst temperature and local gas composition) and the local flow situation.

The local catalyst temperature is needed in order to correctly interpret catalyst activity. Because this temperature is not usually measured, it must be estimated from the measured bulk gas temperature. Accordingly, experimental data from both the fixed bed bench-scale and the micro reactor units, with catalysts SG-A-1, SG-A-2, and SG-B-2, were analyzed. The results indicate that the temperature difference across the gas-catalyst interphase, under synthesis conditions, ranges from less than 1°F to 16°F in the bench-scale unit and from less than 1°F to 6°F in the micro reactors. A similar study on mass transfer was also conducted. The concentration changes of major reactants across the gas-solid interphase were found to be small in all the cases analyzed.

The analysis is based on the assumption that the selectivity and activity are uniform throughout the reactor. This allows the calculation of mass flux across the gas-catalyst interphase from inlet and outlet gas compositions and the space velocity. Deviations from this assumption will be discussed later. With the mass flux given, the temperature and concentration differences can be calculated through the heat and mass balances around a catalyst pellet:

$$h(T - T_o) = h\Delta T = (-\Delta H_i)N_i$$

$$k_c\tilde{\rho}(X_i - X_{io}) = k_c\tilde{\rho}\Delta X_i = N_i - X_{io}\sum_{j=1}^{n} N_j$$

where h(cal/sec - °C - cm^2) and k_c(cm/sec) are the heat and mass transfer coefficients; T_o and T the temperatures (°C) in the bulk gas and on the catalyst surface, X_{io} and X_i the molar fractions of component i in the bulk gas and next to the catalyst surface; $\tilde{\rho}$(g-mole/cc) the molar density; N_i(g-mole/cm^2-sec) the molar flux of component i; and H_i (cal/g-mole) the heat of reaction per mole of component i reacted. The total number of components considered is represented by n.

The heat and mass transfer coefficients in a packed bed are usually arranged in dimensionless forms as Nusselt and Sherwood numbers

$$Nu = \frac{hd_p}{\lambda} \; ; \; Sh = \frac{k_c \, d_p}{D}$$

which are correlated to Reynolds number and Prandtl or Schmidt numbers

$$Re = \frac{d_p \; G}{\mu} \; , \; Pr = \frac{C_p \mu}{\lambda} \; , \; Sc = \frac{\mu}{\rho D}$$

Here d_p is the effective particle diameter in centimeters; G is the superficial mass flow rate in g/cm^2-sec; μ, λ, D, C_p and ρ are respectively the viscosity in g/sec-cm, thermal conductivity in cal/cm-sec°C, diffusivity in cm^2/sec, heat capacity in cal/g-°C, and mass density of the bulk gas in g/cm^3.

Reliable correlations are available at high Reynolds numbers. However, controversy has surrounded the subject of gas-solid heat and mass transfer in packed beds at Reynolds numbers as low as those at which our micro reactor and bench-scale units were operated. The problem was that experimental results were widely scattered over a couple of orders of magnitude and were well below what many sound theories predict. The discrepancy among various experimental data exists to a large extent due to the difficulty involved in direct measurements of transfer driving forces (temperature or concentration difference across solid-gas interphase) which are so small at the bed outlet at low Reynolds numbers that the mean driving forces across the bed can not be determined accurately. To circumvent this difficulty, indirect methods such as effective thermal conductivity measurement(31) and frequency response analysis(32) were often employed to obtain data in this range. Unfortunately, these methods call upon the proposition of an intuitive model for the description of the system, yet the adequacy of the model in representing local transfer processes has not been checked independently. Indeed, the data obtained this way is doubtful as, for example, at Reynolds number about 1, various experiments result in Nusselt numbers ranging from 0.01 to 0.5(31,32), which correspond to heat transfer resistance equivalent to a gas film of thickness ranging from 2 to 100 times the particle diameter, which of course cannot be rationalized by our physical understanding.

Results from various theoretical treatments(33, 34, 35) also differ from each other. This is mainly because of the disagreement on the boundary conditions imposed and the definition of driving forces. When the driving forces, relevant to the present study, are used, these theoretical considerations can be reconciled at least on one common conclusion. That is the Nusselt and Sherwood number should approach a finite limiting value when the Reynolds number approaches zero (stagnant fluid). This limiting value is a function of the void fraction, and in the extreme case, when particles are infinitely far apart, it is well known that the Nusselt number approaches 2. According to the work of Rowe et al(36) and Pfeffer & Happel(33), this limiting value is approximately 13 at a void fraction of 0.4. Based on a different yet more relevant boundary condition, our own analysis gives 23 as the limiting Nu (or Sh) number for the same void fraction. The Nusselt (and Sherwood) number increases with increasing Reynolds number, but only slowly in the low Reynolds number range where our micro reactor and bench-scale units were operated. The Nusselt (and Sherwood) number is only 2% higher than the limiting value at Reynolds number 50, based on present asymptotic expression. In the following analysis, both limiting values for Nusselt and Sherwood were used to estimate the range of temperature and concentration differences between the catalyst and bulk gas stream.

The gas phase viscosities were theoretically calculated through the Chapman-Enskog formula for pure components and then the Wilke method for mixtures. The thermal conductivities were obtained from viscosity data through the Eucken correlation(37). The Chapman-Enskog formula for diffusion was used to estimate the binary diffusivities, with which the effective diffusivity D_{im} of component i in a gas mixture can be evaluated through the Stefan-Maxwell relation(38). Three bench-scale (Unit 225) runs (10, 14, and 15) and six micro reactor runs (in Units 143 and 158) using different catalysts and feed compositions were studied. The effective particle diameters of SG-A-1, SG-A-2, and SG-B-2 are, respectively, 0.115, 0.25, and 0.115 cm. The bench-scale unit, Run 225-10, was carried out in a 50-cc catalyst bed with cross-section area of 3.87 cm^2. Run 225-14 and Run 225-15 used a larger sized reactor of 8.5-cm^2 cross-sectional area and 100-cc and 50-cc bed volumes, respectively. The micro reactor runs were conducted in 10-cc reactors of 1.1-cm^2 cross-sectional area. Other relevant information together with the estimated gas phase properties and the results of heat transfer analysis are listed in Table 27 for the bench-scale and Table 28 for micro reactor unit runs. The interphase temperature differences, ΔT, depends linearly on the heat of reaction (ΔH). The heat of reaction can vary from 25,000 to 40,000 calories per g-mole of CO converted, depending on the product selectivity. In this study a ΔH of 37,500 per g-mole of CO converted was used. For methanation the ΔH is about 52,000 and the ΔT would be 40% higher. The ranges of ΔT were calculated based on the two Nusselt numbers (13 and 23) which are adequate for the description of heat transfer in the Reynolds number range encountered.

In bench-scale unit runs, the calculated ΔT's are relatively small (less than 0.3°F) for Run 225-15 (SG-B-2). This is mainly due to the low catalyst activity of SG-B-2 at the experimental conditions. The ΔT's for Run 225-10 (SG-A-1) and Run 225-15 (SG-A-2) are about 2°F and 6°F, respectively.

TABLE 27

GAS PROPERTIES AND INTERPHASE HEAT TRANSFER IN BENCH-SCALE UNITS (300 PSIG)

Catalyst	SG-A-1						SG-A-2				SG-B-2					
Balance Run CT-225-	10-3		10-3		10-17		14-1		14-6		15-2		15-5		15-7	
Charge, $H_2/CO/CH_4$	3.2/1/0.4		2.1/1/0.3		2.2/1/0.3		2.2/1/0.3		2.2/1/0.3		2.6/1/0.5		2/1/0.5		2.3/1/0.5	
CHSV	3563		3512		2339		490		1003		332		330		325	
Recycle Ratio	8.7		9.4		9.6		12.8		15.6		12.8		13.1		15.7	
% CO Conversion	95.94		61.21		72.06		98.56		96.76		92.65		68.19		75.62	
% H_2 Conversion	77.89		45.83		60.40		95.26		91.01		86.36		79.23		81.15	
N_{CO}, mole/sec-cm^2	1.243×10^{-6}		1.068×10^{-6}		0.823×10^{-6}		0.501×10^{-6}		1.018×10^{-6}		9.446×10^{8}		8.080×10^{-8}		8.082×10^{-8}	
	Inlet	Outlet	Inlet	Outlet	Inlet	Outlet	Inlet	Outlet	Inlet	Outlet	Inlet	Outlet	Inlet	Outlet	Inlet	Outlet
Temperature, °F	482	633	457	629	461	635	515	635	506	635	428	531	427	531	427	532
$\rho \times 10^3$, gm/cc	5.98	5.41	6.95	6.00	7.30	6.36	8.73	8.07	8.61	7.82	8.43	7.80	8.55	7.87	8.04	7.37
$\mu \times 10^4$, gm/sec-cm	1.82	2.00	2.10	2.36	2.05	2.30	1.85	2.00	1.94	2.11	1.79	1.92	1.94	2.08	1.86	2.00
$\lambda \times 10^4$, cal/cm-sec-°C	2.95	3.22	2.96	3.26	2.80	3.14	1.93	2.08	2.08	2.27	1.97	2.09	2.06	2.19	2.13	2.29
Pr	0.51	0.54	0.45	0.47	0.47	0.49	0.65	0.69	0.60	0.63	0.60	0.64	0.56	0.59	0.57	0.60
Re	39.7	36.1	41.0	36.5	30.2	26.9	22.8	21.1	52.4	48.2	9.70	9.03	9.24	8.61	10.5	9.79
$h \times 10^3$, cal/sec-°C-cm^2 Nu=13	33.3	36.4	33.5	36.9	31.7	35.5	10.0	10.8	10.8	11.8	22.3	23.6	23.3	24.8	24.1	25.9
$h \times 10^3$, cal/sec-°C-cm^2 Nu=23	59.0	64.4	59.2	65.2	56.0	62.8	17.8	19.1	19.1	20.9	39.4	41.8	41.2	43.8	42.6	45.8
$\Delta T = 1.8 \times (N_{CO}/h)\, \Delta H$, °F	1.4-2.5	1.3-2.3	1.2-2.2	1.1-2.0	1-1.8	0.9-1.6	1.9-3.4	1.8-3.1	3.6-6.4	3.3-5.8	.16-.29	.15-.27	.13-.23	.12-.22	13-.23	.12-.21
Potential Max. local ΔT, °F	6						16				0.8					

TABLE 28

GAS PROPERTIES AND INTERPHASE HEAT TRANSFER IN MICRO UNITS (200 PSIG)

Catalyst	SG-A-1						SG-B-2									
Balance Run CT	143-51-4		158-88-1		158-91-2		158-99-3		158-99-6		143-58-4		143-58-7		143-59-1	
Charge $H_2/CO/CO_2/CH_4$	2/1/0/0		3/1/2/0		3/1/2/0		1/1/0/0		2/1/0/0		1/1/0/0		1/1/0/0		0.9/1/0.3/3.4	
GHSV	3575		6673		3719		1406		1428		1457		1457		1511	
% CO Conversion	99		78		83		39		71		34		38		32	
% H_2 Conversion	63		51		52		75		79		68		79		85	
N_{co}, mole/sec-cm^2	1.988×10^{-6}		1.462×10^{-6}		8.668×10^{-6}		1.448×10^{-7}		4.250×10^{-7}		3.115×10^{-7}		3.481×10^{-7}		1.086×10^{-7}	
	Inlet	Outlet	Inlet	Outlet	Inlet	Outlet	Inlet	Outlet	Inlet	Outlet	Inlet	Outlet	Inlet	Outlet	Inlet	Outlet
Temperature, °F	610	637	608	639	608	634	490	518	486	515	492	506	510	525	518	528
$\rho \times 10^3$, gm/cc	3.20	5.47	6.11	7.71	6.11	7.71	5.06	7.21	3.64	6.26	5.05	7.04	4.96	7.34	5.71	6.47
$\mu \times 10^4$, gm/sec-cm	2.55	2.20	2.69	2.58	2.69	2.55	2.52	2.24	2.35	1.98	2.52	2.26	2.55	2.26	2.07	2.02
$\lambda \times 10^4$, cal/cm-sec-°C	4.02	2.66	2.81	2.05	2.81	2.02	2.82	1.58	3.69	1.87	2.82	1.69	2.86	1.51	1.86	1.49
Pr	0.42	0.50	0.40	0.49	0.40	0.50	0.42	0.61	0.42	0.59	0.42	0.57	0.42	0.63	0.65	0.77
Re	0.33	0.38	1.11	1.16	0.62	0.66	0.48	0.54	0.37	0.45	0.50	0.56	0.49	0.56	0.73	0.75
$h \times 10^3$, cal/sec-°C-cm^2 Nu=13	44.6	29.5	31.2	22.7	31.2	22.5	31.3	17.5	41.0	20.6	31.3	18.8	31.8	16.7	20.7	16.6
Nu=23	80.2	53.1	56.1	40.9	56.1	40.4	56.3	31.5	73.7	37.4	56.3	33.8	57.1	30.1	37.2	29.7
$\Delta T = 1.8 \times (N_{co}/h)\ H$, °F	1.7-3.0	2.5-4.5	1.8-3.2	2.4-4.3	1.0-1.9	1.4-2.6	0.4-0.7	0.7-1.3	0.4-0.7	0.8-1.4	0.4-0.7	0.6-1.1	0.4-0.7	0.8-1.4	0.2-0.4	0.2-0.4
Adjusted local ΔT, °F	3.1-5.6	1.2 2.8	2.7-4.8	1.5-2.7	1.5-2.9	0.9-1.6	0.6-1.0	0.4-0.8	0.8-1.3	0.4-0.6	0.6-1.0	0.4-0.8	0.6-1.1	0.5-0.9	0.3-0.6	0.1-0.2

The higher interphase temperature difference with SG-A-2, compared with SG-A-1, is attributed to lower space velocity and larger catalyst particle size. The temperature differences based on both reactor inlet and reactor outlet conditions were estimated. There is little difference between these two.

The above results were based on the average conversion rate, as the selectivity and activity were assumed uniform throughout the reactor. Since the conversion profile along an adiabatic bench-scale reactor is similar to the temperature profile, deviations of local rate from the average can be roughly estimated from the latter. The ratio of a local conversion rate to the average rate, is approximately equal to the ratio of the local slope of the temperature profile to the slope of the line connecting the inlet and outlet temperatures. Figure 30 depicts several axial temperature profiles. For material balances 10-2 and 15-2, the highest conversion rates were achieved at the reactor exit, and were about 2 and 2.5 times the average rates, respectively. For material balance 14-1, the local rates do not differ too much from the average rate. As ΔT is linearly proportioned to the conversion rate, ΔT's at the outlet for material balances 10-3, 15-2 should be corrected by the factors 2 and 2.5 respectively. Thus, the potential maximum local ΔT in the bench-scale unit might be as high as 2.5 times the ΔT's obtained by using the average rate. These potential ΔT's for various catalysts are also given in Table 27.

In micro reactors the temperature differences between the catalyst and bulk gas stream for SG-B-2 catalyst are again found to be smaller than those for SG-A-1 catalyst as shown in Table 28. In contrast to bench-scale unit are the distinct differences between inlet and outlet gas compositions and properties in micro reactor units. This is because of the absence of recycle. Since the concentrations of reactants change a great deal from inlet to outlet in micro reactors, it is expected that the local reaction rate at the inlet would be higher than the average rate. Indeed if the reaction is assumed to have first order dependence on the reactant concentration, it can be shown that

$$\frac{r_{in}}{r_{av}} = - \frac{\ln(1-Y)}{Y}$$

$$\frac{r_{out}}{r_{av}} = - \frac{(1-Y)\ln(1-Y)}{Y}$$

where r_{in}, r_{out} and r_{av} are, respectively, the inlet, outlet, and average reaction rates and Y is the conversion. Based on this simple assumption, the adjusted local ΔT's are listed in Table 28. The maximum adjustment gives a ΔT about twice as large.

FIGURE 30

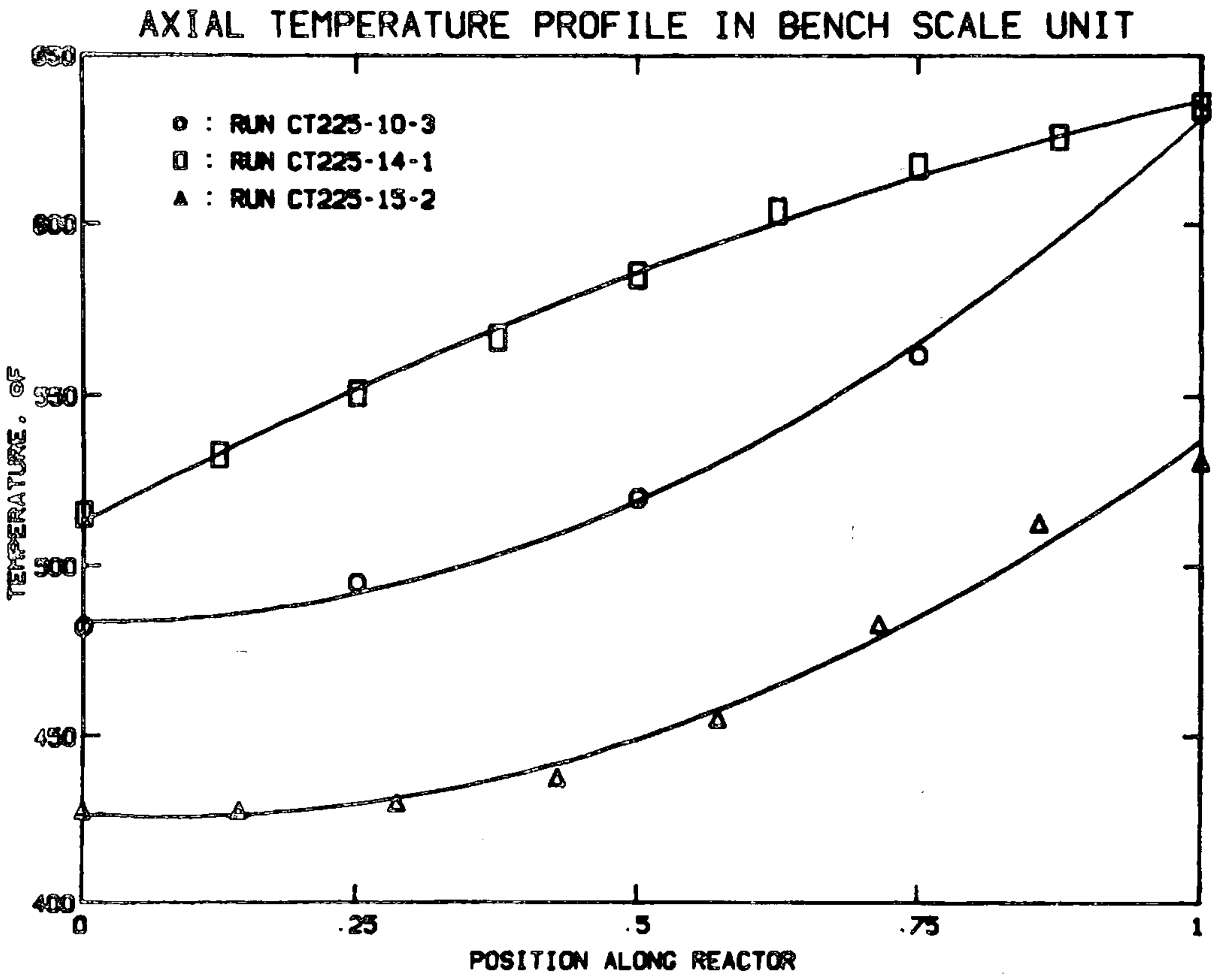
AXIAL TEMPERATURE PROFILE IN BENCH SCALE UNIT
o : RUN CT225-10-3
□ : RUN CT225-14-1
Δ : RUN CT225-15-2
TEMPERATURE, °F
650
600
550
500
450
400
0
.25
.5
.75
1
POSITION ALONG REACTOR

The results of mass transfer analysis based on Sh=13 are listed in Table 29 and Table 30 for bench-scale and micro reactor units, respectively. The concentration differences across the gas-catalyst interphase are expressed as the molar fraction differences, ΔX_i's. The ΔX's for components CO and H_2 are very small in comparison with the respective molar fractions X_i's in all the cases studied. If Sh=23 is used, the ΔX's are even smaller. It can thus be concluded that the bulk gas stream composition adequately represents the composition at the catalyst surface.

2. Heat Loss from Fixed-Bed Bench-Scale Unit

As mentioned earlier, a large amount of heat is released during synthesis gas conversion. This heat has to be effectively removed from the reactor to avoid temperature run-away. In the fixed-bed bench-scale unit, the reactor was designed to simulate adiabatic operation. All the reaction heat was to be removed by the recycled gas. Estimations of heat loss from experimental data indicate that the fixed bed bench-scale unit was indeed operated close to adiabatic conditions.

The heat loss from a reactor can be calculated from the enthalpy difference between reactor effluent and feed. For an adiabatic reactor, this difference should be zero, and the reaction heat results in a higher or lower effluent temperature, depending on whether the reactions occurring are exothermic or endothermic. This effluent temperature is called the adiabatic temperature of the reacting stream. For an actual reactor, an exit temperature lower than the adiabatic temperature, indicates a heat loss to ambient.

To estimate the enthalpy of a feed or effluent stream, a detailed composition breakdown is needed. For the current study, the compositions are divided into 59 component lumps, including 55 components for the C_1 to C_{11} hydrocarbons and four components for the inorganics H_2O, H_2, CO, and CO_2.

Raw experimental data were screened before detailed analysis. Only those data whose C-H-O atomic balances in the net product stream (i.e., without recycle) were within 2% of those of the fresh feed stream were used. Furthermore, slight adjustments in product composition were made so that an exact C-H-O balance between feed and product stream could be attained. In adjusting the raw data, the (H_2+CO) conversion, hydrocarbon selectivity, and ratio of oxygen rejection as H_2O and CO_2 for all experiments, were maintained the same.

Four fixed bed material balances using SG-A-2 and SG-B-2 catalysts were thus chosen for this study. The calculated adiabatic temperatures, together with the measured reactor outlet temperature and other pertinent information, are listed in Table 31. The result

TABLE 29

INTERPHASE MASS TRANSFER IN BENCH SCALE UNITS (Sh=13)

Run CT-225-	10-3		14-1		15-2	
Catalyst	SG-A-1		SG-A-2		SG-B-2	
Component-CO						
N_i, mole/sec-cm^2	1.234×10^{-6}		0.501×10^{-6}		0.945×10^{-7}	
	Inlet	Outlet	Inlet	Outlet	Inlet	Outlet
D_{im}, cm^2/sec.	0.0349	0.0451	0.0281	0.0343	0.0221	0.0267
Sc	0.87	0.82	0.76	0.72	0.96	0.92
k_c, cm/sec.	3.95	5.10	1.47	1.78	2.50	3.01
X_i	0.0501	0.0302	0.0389	0.0194	0.1236	0.1106
$\Delta X_i \times 10^4$	0.69	5.3	6.6	6.3	0.55	0.52
Component-H_2						
N_i, mole/sec-cm^2	3.214×10^{-6}		1.086×10^{-6}		2.252×10^{-7}	
	Inlet	Outlet	Inlet	Outlet	Inlet	Outlet
D_{im}, cm^2/sec.	0.0820	0.1062	0.0865	0.1055	0.0764	0.0922
Sc	0.37	0.35	0.25	0.24	0.28	0.27
k_c, cm/sec.	9.27	12.0	4.50	5.50	8.65	10.4
X_i	0.5059	0.4731	0.1976	0.1597	0.2621	0.2301
$\Delta X_i \times 10^4$	3.9	3.7	4.2	4.0	0.39	0.37

TABLE 30

INTERPHASE MASS TRANSFER IN MICRO UNITS (Sh=13)

Run CT-	143-51-4		158-99-6		143-58-4	
Catalyst	SG-A-1		SG-B-2		SG-B-2	
Component-CO						
N_i, mole/sec-cm^2	1.988×10^{-6}		4.250×10^{-7}		3.115×10^{-7}	
	Inlet	Outlet	Inlet	Outlet	Inlet	Outlet
D_{im}, cm^2/sec	0.0592	0.0619	0.0320	0.0340	0.0098	0.0101
Sc	1.35	0.65	2.02	0.93	5.09	3.19
k_c, cm/sec	6.70	6.99	3.62	3.84	1.11	1.14
X_i	0.3333	0.0058	0.3333	0.1716	0.5000	0.4670
$\Delta X_i \times 10^4$	5.6	9.6	1.3	2.3	1.1	1.5
Component-H_2						
N_i, mole/sec-cm^2	2.530×10^{-6}		9.338×10^{-7}		6.230×10^{-7}	
	Inlet	Outlet	Inlet	Outlet	Inlet	Outlet
D_{im}, cm^2/Sec.	0.1426	0.1491	0.1308	0.1384	0.1334	0.1370
Sc	0.56	0.27	0.49	0.23	0.37	0.23
k_c, cm/sec.	16.1	16.9	14.8	15.7	15.1	15.5
X_i	0.6667	0.4321	0.6667	0.2603	0.5000	0.2264
$\Delta X_i \times 10^4$	1.7	2.9	0.82	1.4	0.70	0.98

TABLE 31

REACTOR OUTLET TEMPERATURES VS CALCULATED ADIABATIC TEMPERATURES IN FIXED BED BENCH-SCALE UNIT

	Catalyst			
	SG-A-2	SG-B-2		
Run CT 225-	14-7	15-2	15-5	15-14
Fresh Feed, $H_2/CO/CH_4$	2/1/0.3	2.6/1/0.5	2/1/0.5	2.2/1/0.5
GHSV, hr^{-1}	966	332	330	332
Recycle Ratio	15.9	12.8	13.1	13.8
H_2+CO Conversion, mole %	92.3	88.1	75.6	69.5
Reactor Temperature, °F				
Inlet	500	430	424	424
Outlet	637	531	531	527
Adiabatic Temperature, °F	601	536	530	527